

Super-acceleration as Signature of Dark Sector Interaction

Subinoy Das^{1,2}, Pier Stefano Corasaniti¹ and Justin Khoury³

¹*ISCAP, Columbia University, New York, NY 10027, USA*

²*Center for Cosmology and Particle Physics, Department of Physics,
New York University, New York, NY 10003, USA*

³*Center for Theoretical Physics, Massachusetts Institute of Technology, Cambridge, MA 02139, USA*

We show that an interaction between dark matter and dark energy generically results in an effective dark energy equation of state of $w < -1$. This arises because the interaction alters the redshift-dependence of the matter density. An observer who fits the data treating the dark matter as non-interacting will infer an effective dark energy fluid with $w < -1$. We argue that the model is consistent with all current observations, the tightest constraint coming from estimates of the matter density at different redshifts. Comparing the luminosity and angular-diameter distance relations with Λ CDM and phantom models, we find that the three models are degenerate within current uncertainties but likely distinguishable by the next generation of dark energy experiments.

I. INTRODUCTION

Nature would be cruel if dark energy were a cosmological constant. Unfortunately this daunting possibility is increasingly likely as observations converge towards an equation of state of $w = -1$. Combining galaxy, cosmic microwave background (CMB) and Type Ia supernovae (SNIa) data, Seljak *et al.* [1] recently found $-1.1 \lesssim w \lesssim -0.9$ at 1σ . On the one hand, a cosmological constant is theoretically simple as it involves only one parameter. However, observations would offer no further guidance to explain its minuteness, whether due to some physical mechanism or anthropic reasoning [2].

A more fertile outcome is $w \neq -1$. This implies dynamics — the vacuum energy is changing in a Hubble time — and hence, new physics. A well-studied candidate is quintessence [3, 4], a scalar field ϕ rolling down a self-interaction potential $V(\phi)$. Its equation of state,

$$w_\phi = \frac{\dot{\phi}^2/2 - V(\phi)}{\dot{\phi}^2/2 + V(\phi)}, \quad (1)$$

can be $< -1/3$ for sufficiently flat $V(\phi)$ and thus lead to cosmic speed-up. Whether dark energy is quintessence or something else, this case offers hope that further observations, either cosmological or in the solar system, may unveil the underlying microphysics of the new sector.

An even more exciting possibility is $w < -1$. In fact there are already indications of this [5, 6] from various independent analyses of the “Gold” SNIa dataset [7]. Moreover, by constraining redshift parameterizations of $w(z)$ they also exclude that this could result from assuming a constant w [8]. The $w < -1$ regime would rule out quintessence since $w_\phi \geq -1$ (see Eq. (1)), as well as most dark energy models.

Devising consistent models with $w < -1$ has proven to be challenging. Existing theories generally involves ghosts, such as phantom models [9], resulting in instabilities and other pathologies [10]. Fields with non-minimal couplings to gravity, such as Brans-Dicke theory, can mimic $w < -1$ [11]. However, solar-system constraints render the Brans-Dicke scalar field nearly inert, thereby

driving w indistinguishably close to -1 . Another proposal is that the extra dimming of SNIa necessary for $w < -1$ results from photon-axion conversion [12].

In this paper we show that $w < -1$ naturally arises if quintessence interacts with dark matter. The mechanism is simple. Due to the interaction, the mass of dark matter particles depends on ϕ . Consequently, in the recent past the dark matter energy density redshifts more slowly than the usual a^{-3} , which, for fixed present matter density, implies a smaller matter density in the past compared to normal cold dark matter (CDM).

An observer unaware of the interaction and fitting the data assuming normal CDM implicitly ascribes this dark matter deficit to the dark energy. The effective dark energy fluid thus secretly receives two contributions: the quintessence part and the deficit in dark matter. The latter is growing in time, therefore causing the effective dark energy density to also increase with time, hence $w < -1$.

Treating dark matter as non-interacting is a *sine qua non* for inferring $w < -1$. There are no wrong-sign kinetic terms in our model — in fact the combined dark matter plus dark energy fluid satisfies $w > -1$. Hence the theory is well-defined and free of instabilities.

Interacting dark matter/dark energy models have been studied in various contexts [13, 14, 15, 16, 17, 18]. Huey and Wandelt [19] first realized that coupled dark matter/quintessence can yield an effective $w < -1$. However, the dynamics in [19] are such that DM density becomes negligibly small for $z \gtrsim 1$, thereby forcing the addition of a second non-interacting DM component. In contrast, our model involves a single (interacting) DM component.

Given the lack of competing consistent models, we advocate that measuring $w < -1$ would hint at an interaction in the dark sector. More accurate observations could then search for direct evidence of this interaction. For instance, we show that the extra attractive force between dark matter particles enhances the growth of perturbations and leads to a few percent excess of power on small scales. Other possible signatures are discussed below.

II. DARK SECTOR INTERACTION

Consider a quintessence scalar field ϕ which couples to the dark matter via, *e.g.*, a Yukawa-like interaction

$$f(\phi/M_{\text{Pl}})\bar{\psi}\psi, \quad (2)$$

where f is an arbitrary function of ϕ and ψ is a dark matter Dirac spinor. In order to avoid constraints from solar-system tests of gravity, we do not couple ϕ to baryons. See [15], however, for an alternative approach.

In the presence of this dark-sector interaction, the energy density in the dark matter no longer redshifts as a^{-3} but instead scales as

$$\rho_{\text{DM}} \sim \frac{f(\phi/M_{\text{Pl}})}{a^3}. \quad (3)$$

This can be easily understood since the coupling in Eq. (2) implies a ϕ -dependent mass for the dark matter particles scaling as $f(\phi/M_{\text{Pl}})$. Since the number density redshifts as a^{-3} as usual, Eq. (3) follows.

Thus the Friedmann equation reads

$$3H^2 M_{\text{Pl}}^2 = \frac{\rho_{\text{DM}}^{(0)}}{a^3} \frac{f(\phi/M_{\text{Pl}})}{f_0} + \rho_\phi, \quad (4)$$

where $f_0 = f(\phi_0/M_{\text{Pl}})$ with ϕ_0 the field value today, and

$$\rho_\phi = \frac{1}{2}\dot{\phi}^2 + V(\phi) \quad (5)$$

is the scalar field energy density. With $a = 1$ today, $\rho_{\text{DM}}^{(0)}$ is identified as the present dark matter density.

Meanwhile, the scalar field evolution is governed by

$$\ddot{\phi} + 3H\dot{\phi} = -V_{,\phi} - \frac{\rho_{\text{DM}}^{(0)}}{a^3} \frac{f_\phi}{f_0}. \quad (6)$$

This differs from the usual Klein-Gordon equation for quintessence models by the last term on the right-hand side, arising from the interaction with dark matter.

The standard approach to constraining dark energy with experimental data assumes that it is a non-interacting perfect fluid, fully described by its equation of state, w_{eff} . Given some $w_{\text{eff}}(z)$, the evolution of the dark energy density is then determined by the energy conservation equation:

$$\frac{d\rho_{\text{DE}}^{\text{eff}}}{dt} = -3H(1+w_{\text{eff}})\rho_{\text{DE}}^{\text{eff}}. \quad (7)$$

Meanwhile, the dark matter is generally assumed to be non-interacting CDM, resulting in the Friedmann equation

$$3H^2 M_{\text{Pl}}^2 = \frac{\rho_{\text{DM}}^{(0)}}{a^3} + \rho_{\text{DE}}^{\text{eff}}. \quad (8)$$

An observer applying these assumptions to our model would infer an effective dark energy fluid with

$$\rho_{\text{DE}}^{\text{eff}} \equiv \frac{\rho_{\text{DM}}^{(0)}}{a^3} \left[\frac{f(\phi/M_{\text{Pl}})}{f(\phi_0/M_{\text{Pl}})} - 1 \right] + \rho_\phi, \quad (9)$$

obtained by comparing Eqs. (4) and (8). The end result is to effectively ascribe part of the dark matter to dark energy. Notice that today the first term vanishes, hence the effective dark energy density coincides with ρ_ϕ . In the past, however, $\phi \neq \phi_0$, and the two differ. In particular, we will find that the time-dependence of $\rho_{\text{DE}}^{\text{eff}}$ can be such that $w_{\text{eff}} < -1$.

To show this explicitly requires an expression for w_{eff} . Taking the time derivative of Eq. (9) and substituting the scalar equation of motion, Eq. (6), we obtain

$$\frac{d\rho_{\text{DE}}^{\text{eff}}}{dt} = -3H \left\{ \frac{\rho_{\text{DM}}^{(0)}}{a^3} \left[\frac{f(\phi/M_{\text{Pl}})}{f(\phi_0/M_{\text{Pl}})} - 1 \right] + (1+w_\phi)\rho_\phi \right\}. \quad (10)$$

Comparing with Eq. (7) allows us to read off w_{eff} :

$$1+w_{\text{eff}} = \frac{1}{\rho_{\text{DE}}^{\text{eff}}} \left\{ \left[\frac{f(\phi/M_{\text{Pl}})}{f(\phi_0/M_{\text{Pl}})} - 1 \right] \frac{\rho_{\text{DM}}^{(0)}}{a^3} + (1+w_\phi)\rho_\phi \right\}. \quad (11)$$

Now suppose that the dynamics of ϕ are such that $f(\phi/M_{\text{Pl}})$ increases in time. This occurs in a wide class of models, as we will see in Section III. In this case,

$$x \equiv -\frac{\rho_{\text{DM}}^{(0)}}{a^3\rho_\phi} \left[\frac{f(\phi/M_{\text{Pl}})}{f(\phi_0/M_{\text{Pl}})} - 1 \right] \geq 0 \quad (12)$$

for all times until today, with equality holding at the present time. It is straightforward to show that w_{eff} takes a very simple form when expressed in terms of x :

$$w_{\text{eff}} = \frac{w_\phi}{1-x}. \quad (13)$$

This is our main result. Since $x = 0$ today, one has $w_{\text{eff}}^{(0)} = w_\phi^{(0)}$, which is greater than or equal to -1 . In the past, however, $x > 0$. Moreover, for sufficiently flat potentials, $w_\phi \approx -1$. Hence it is possible to have $w_{\text{eff}} < -1$ in the past. This is shown explicitly in Fig. 1 for a fiducial case: $f(\phi/M_{\text{Pl}}) = \exp(\beta\phi/M_{\text{Pl}})$ and $V(\phi) = M^4(M_{\text{Pl}}/\phi)^\alpha$.

III. QUINTESSENCE DYNAMICS

We now come back to the equation of motion for ϕ , Eq. (6), and demonstrate that its dynamics can lead to $w_{\text{eff}} < -1$. The scalar potential $V(\phi)$ is assumed to satisfy the tracker condition [20],

$$\Gamma \equiv \frac{V_{,\phi\phi}V}{V_{,\phi}^2} > 1. \quad (14)$$

For an exponential potential, $\Gamma = 1$, while $\Gamma = 1 + \alpha^{-1}$ for $V(\phi) \sim \phi^{-\alpha}$. Moreover, we take the coupling function f to be monotonically increasing.

Without coupling to dark matter, the scalar field would run off to infinite values. Here, however, the interaction

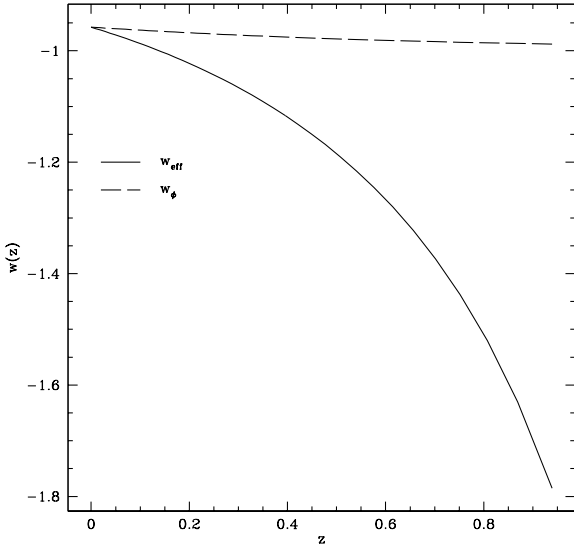


FIG. 1: Redshift evolution of w_{eff} (solid line) and w_ϕ (dash line). As advocated, $w_{\text{eff}} < -1$ in the recent past due to the interaction with the dark matter.

has a stabilizing effect since ϕ wants to minimize the effective potential

$$V^{\text{eff}} = V(\phi) + \frac{\rho_{\text{DM}}^{(0)}}{a^3} \frac{f(\phi/M_{\text{Pl}})}{f(\phi_0/M_{\text{Pl}})}. \quad (15)$$

Indeed, it is easily seen that the right-hand side of Eq. (6) is just $-V_\phi^{\text{eff}}$. Similar stabilization mechanisms have been explored in other contexts, such as so-called VAMPS scenarios [21], string moduli [22, 23], chameleon cosmology [15, 16], interacting neutrino/dark energy models [18], and other interacting dark matter/dark energy models [19, 24], to name a few.

Having ϕ at the minimum of the effective potential is an attractor solution [16]: as the dark matter density redshifts due to cosmic expansion, ϕ adiabatically shifts to larger field values, always minimizing V^{eff} . This is because the period of oscillations about the minimum, m^{-1} , is much shorter than a Hubble time, *i.e.*, $m \gg H$. We show this for the present epoch, leaving the proof for all times as a straightforward exercise.

The mass of small fluctuations about the minimum is given as usual by

$$m^2 = V_{,\phi\phi}^{\text{eff}} = \frac{\rho_{\text{DM}}^{(0)}}{a^3} \frac{f_{,\phi\phi}}{f_0} \left\{ 1 + \frac{f_{,\phi}^2}{f_{,\phi\phi} f} \frac{\Gamma}{V} \frac{\rho_{\text{DM}}^{(0)}}{a^3} \frac{f}{f_0} \right\}, \quad (16)$$

where we have substituted Γ using its definition, Eq. (14). Evaluating this today, and noting that $\rho_{\text{DM}}^{(0)} = 3H_0^2 M_{\text{Pl}}^2 \Omega_{\text{DM}}^{(0)}$ and $V(\phi_0) < 3H_0^2 M_{\text{Pl}}^2 \Omega_{\text{DE}}^{(0)}$, we find

$$\frac{m_0^2}{H_0^2} > 3\Omega_{\text{DM}}^{(0)} M_{\text{Pl}}^2 \left(\frac{f_{,\phi\phi}}{f} \right)_0 \left\{ 1 + \Gamma \left(\frac{f_{,\phi}^2}{f_{,\phi\phi} f} \right)_0 \frac{\Omega_{\text{DE}}^{(0)}}{\Omega_{\text{DM}}^{(0)}} \right\}. \quad (17)$$

The right hand side is greater than unity for $M_{\text{Pl}}^2 f_{,\phi\phi}/f \gtrsim 1$. In addition, as we will see later, $\Gamma \gg 1$ for consistency with observations of large-scale structure. These conditions guarantee that fluctuations about the minimum of the effective potential are small at the present time. For concreteness, let us evaluate this in the case of $f(\phi) = \exp(\beta\phi/M_{\text{Pl}})$ and $V(\phi) = M^4(M_{\text{Pl}}/\phi)^\alpha$:

$$\frac{m_0^2}{H_0^2} > 3\beta^2 \Omega_{\text{DM}}^{(0)} \left(1 + \frac{\alpha + 1}{\alpha} \frac{\Omega_{\text{DM}}^{(0)}}{\Omega_{\text{DE}}^{(0)}} \right). \quad (18)$$

This is indeed larger than unity for $\alpha \lesssim 1$ and $\beta \gtrsim \mathcal{O}(1)$, the latter corresponding to a gravitational-strength interaction between dark matter and dark energy.

Next we show that the field is slow-rolling along this attractor solution. The proof is again straightforward. Differentiating the condition at the minimum, $V_{,\phi}^{\text{eff}} = 0$, with respect to time, we obtain

$$\dot{\phi} = \frac{3H}{m^2} \frac{\rho_{\text{DM}}^{(0)}}{a^3} \frac{f_{,\phi}}{f_0} = -\frac{3H}{m^2} V_{,\phi}, \quad (19)$$

where in the last step we have used $V_{,\phi}^{\text{eff}} = 0$. Thus,

$$\frac{\dot{\phi}^2}{2V} = \frac{9H^2}{2m^4} \frac{V_{,\phi}^2}{V} < \frac{9H^2}{2m^2} \frac{1}{\Gamma}. \quad (20)$$

Since $m > H$ along the attractor, and since $\Gamma \gg 1$ as mentioned earlier, Eq. (20) implies that ϕ has negligible kinetic energy compared to potential energy, which is the definition of slow-roll.

The slow-roll property has many virtues. First of all, it implies that our attractor solution is different than that derived by Amendola and collaborators [14]. In their case, during the matter-dominated era, the scalar field kinetic energy dominates over the potential energy and remains a fixed fraction of the critical density. This significantly alters the growth rate of perturbations. Microwave background anisotropy then constrains the dark matter-dark energy coupling to be less than gravitational strength: $\beta < 0.1$ for $f(\phi) = \exp(\beta\phi/M_{\text{Pl}})$. In our case, as we will see in Sec. V C, slow-roll implies a nearly identical growth rate to that in CDM models, even in the interesting regime $\beta \gtrsim 1$.

More importantly, slow-roll means $w_\phi \approx -1$. As argued below Eq. (13), this facilitates obtaining $w_{\text{eff}} < -1$.

In essence, slow-roll is enhanced by the dark matter interaction term in Eq. (6) which acts to slow down the field. To see this explicitly, note that in usual quintessence models (without dark matter interaction), slow-roll is achieved in the large Γ limit, for which

$$\frac{\dot{\phi}^2}{2V} \approx \frac{1}{4\Gamma}. \quad (21)$$

Comparison with Eq. (20) shows that this ratio is further suppressed by $H^2/m^2 \ll 1$ in our case.

The attractor solution described here has a large basin of attraction. The covariant form of Eq. (6) involves T_μ^μ ,

the trace of the stress tensor of all fields coupled to ϕ . These do not exclusively consist of DM. For instance, in a supersymmetric model where the DM is the lightest supersymmetric particle, ϕ could conceivably couple to a host of superpartners. Deep in the radiation-dominated era, the T_μ^μ source term is generally negligible compared to the Hubble damping term, $3H\dot{\phi}$. However, they become comparable for about a Hubble time whenever a particle species coupled to ϕ becomes non-relativistic [22], therefore driving ϕ towards the minimum of its effective potential. This provides an efficient mechanism for reaching the attractor [16].

IV. AN EXPLICIT EXAMPLE

In this Section we illustrate our mechanism within a specific model. We consider an inverse power-law potential, $V(\phi) = M^4(M_{\text{Pl}}/\phi)^\alpha$, where the mass scale M is tuned to $\sim 10^{-3}$ eV in order for acceleration to occur at the present epoch. This potential is a prototypical example of a tracker potential in quintessence scenarios. Its runaway form is in harmony with non-perturbative potentials for moduli in supergravity and string theories.

The coupling function is chosen to be $f(\phi) = \exp(\beta\phi/M_{\text{Pl}})$. The exponential form is generic in dimensional reduction in string theory where ϕ measures the volume of extra dimensions. Moreover, β is expected to be of order unity, corresponding to gravitational strength.

In this case, the condition at the minimum reads

$$-\frac{\alpha M^4 M_{\text{Pl}}^\alpha}{\phi^{\alpha+1}} + \frac{\beta}{M_{\text{Pl}}} \frac{\rho_{\text{DM}}^{(0)}}{a^3} e^{\beta(\phi-\phi_0)/M_{\text{Pl}}} = 0. \quad (22)$$

Evaluating this today, and noting that $V_0 \approx 3H_0^2 M_{\text{Pl}}^2 \Omega_{\text{DE}}^{(0)}$ because of slow-roll, we obtain

$$\frac{\phi_0}{M_{\text{Pl}}} \approx \frac{\alpha}{\beta} \frac{\Omega_{\text{DE}}^{(0)}}{\Omega_{\text{DM}}^{(0)}}. \quad (23)$$

Equations (22) and (23) combine to provide a simple expression for the redshift-evolution of ϕ as it follows the minimum of the effective potential:

$$\left(\frac{\phi}{\phi_0}\right)^{\alpha+1} = (1+z)^{-3} e^{\beta(\phi_0-\phi)/M_{\text{Pl}}}. \quad (24)$$

Next we calculate the resulting effective equation of state. To do so, we first need an expression for ρ_ϕ as a function of redshift. Notice that in the slow-roll approximation, $\rho_\phi \approx V(\phi)$. This does not imply, however, that $\rho_\phi \approx \text{const.}$, since ρ_ϕ does not obey the usual conservation equation. Using Eq. (22), we instead have

$$\rho_\phi \approx \frac{V}{V_{,\phi}} V_{,\phi} = \frac{\beta}{\alpha} \frac{\phi}{M_{\text{Pl}}} \frac{\rho_{\text{DM}}^{(0)}}{a^3} e^{\beta(\phi-\phi_0)/M_{\text{Pl}}}. \quad (25)$$

Substituting this and Eq. (25) in the definition of x given in Eq. (12), we arrive at

$$x = \frac{\Omega_{\text{DM}}^{(0)} \phi_0}{\Omega_{\text{DE}}^{(0)} \phi} \left\{ \exp \left[\alpha \frac{\Omega_{\text{DE}}^{(0)}}{\Omega_{\text{DM}}^{(0)}} \left(1 - \frac{\phi}{\phi_0} \right) \right] - 1 \right\}. \quad (26)$$

This shows explicitly that x is a positive, monotonically increasing function of z which vanishes today. Moreover, since the field is slow-rolling, we have $w_\phi \approx -1$. Therefore, Eq. (13) implies

$$w_{\text{eff}} \approx -\frac{1}{1-x} \leq -1, \quad (27)$$

with the approximate equality holding today. Hence this yields an effective dark energy fluid with $w < -1$ in the recent past.

Note from Eq. (26) that $x = 1$ at some time in the past, implying that $|w_{\text{eff}}|$ momentarily diverges and then becomes positive again at higher redshifts. This is because $\rho_{\text{DE}}^{\text{eff}}$ eventually becomes negative, at which point the effective dark energy fluid has both negative pressure and energy density. As z increases further and x becomes large, one has $w_{\text{eff}} \approx 0$, and the fluid behaves like dust.

In Fig. 1 we plot the redshift evolution of w_{eff} and w_ϕ for $\alpha = 0.2$, $\beta = 1$ and $\Omega_{\text{DE}}^{(0)} = 0.7$. (As will be discussed in the next Section, a small value for α is required for consistency with large-scale structure observations.) While w_ϕ remains bounded from below by -1, w_{eff} is less than -1 for $z \gtrsim 0.1$, as claimed above.

The evolution of $w_{\text{eff}}(z)$ shown in Fig. 1 is consistent with the observational limits on redshift dependent parameterizations of the dark energy equation of state [6]. One way to see this is to consider the weighted average

$$\bar{w}_{\text{eff}} \equiv \frac{\int \Omega_{\text{eff}}(a) w_{\text{eff}}(a) da}{\int \Omega_{\text{eff}}(a) da}, \quad (28)$$

where the integral runs from $z = 0$ up to the maximum redshift of current SN Ia data, $z \sim 1.5$. This gives $\bar{w}_{\text{eff}} \approx -1.1$, which lies within the allowed range of w found in [1]. Note that while Fig. 1 was derived using the above analytical expressions, we have checked these against numerical solutions of the equations of motion and found very good agreement.

V. OBSERVATIONAL CONSTRAINTS AND CONSEQUENCES

We have shown that the interaction between quintessence and dark matter can mimic the cosmology of a phantom fluid. In this Section we discuss some observational consequences of this scenario and argue that it is consistent with current observations. At the level of homogeneous cosmology this is certainly true, as long as parameters are chosen such that w_{eff} lies within the allowed range. We argue that this is also the case when considering inhomogeneities, at least at the linear level.

The main effect here is the fifth force between dark matter particles mediated by ϕ , which enhances the growth rate of density perturbations.

A rigorous comparison with observations would require a full likelihood analysis including a host of cosmological probes, which is beyond the scope of this paper. We instead contend ourselves with a simplified (and perhaps more conservative) analysis to derive general constraints. As in Sec. IV, we focus on an exponential coupling function and inverse power-law potential.

A. Mass estimates from large-scale structure

The tightest constraint comes from various estimates of the dark matter density at different redshifts. Since the dark matter redshifts more slowly than a^{-3} in our model, then for fixed present matter density this implies a smaller matter density in the past compared to a CDM model. Indeed, at early times ($\phi \ll \phi_0$), the matter density differs from that of a usual dust CDM model by

$$\frac{\rho_{\text{DM}}}{\rho_{\text{CDM}}} \rightarrow e^{-\beta\phi_0/M_{\text{Pl}}} = \exp\left(-\alpha \frac{\Omega_{\text{DE}}^{(0)}}{\Omega_{\text{DM}}^{(0)}}\right), \quad (29)$$

where in the last step we have used Eq. (23).

It is reasonable to assume that this ratio cannot deviate too much from unity, for otherwise we risk running into conflict with estimates of the matter density at various redshifts, *e.g.* from galaxy counts, Lyman- α forest, weak lensing etc. This is supported by the fact that the allowed range of $\Omega_{\text{DM}}^{(0)}$ is almost independent of the specifics of the dark energy, as derived from a general analysis [6, 25] of the combined SNIa “Gold” data [7], Wilkinson Anisotropy Microwave Probe (WMAP) power spectra [26] and Two-Degree Field (2dF) galaxy survey [27]. In particular $0.23 \lesssim \Delta\Omega_{\text{DM}}^{(0)} \lesssim 0.33$ at 2σ (see also [1, 28]). Substituting $\Omega_{\text{DM}}^{(0)} = 0.33$ in Eq. (29), we obtain

$$\alpha \lesssim 0.2. \quad (30)$$

Thus dark matter density estimates require the scalar field potential to be sufficiently flat, thereby making the attractor behavior and slow-roll condition discussed in Sec. III more easily satisfied.

Equation (29) shows that ρ_{DM} redshifts like normal CDM (*i.e.*, $\rho_{\text{DM}} \sim a^{-3}$) for most of the cosmological history, except in the recent past. This is crucial in satisfying constraints on $\Omega_{\text{DM}}^{(0)}$ and traces back to our choice of inverse power-law potential. In contrast, the exponential potential studied in [19] has a very different attractor solution. In this case, dark energy remains a constant fraction of the total energy density and modifies the DM equation of state at all redshift. This in turn renders the matter density negligibly small for $z \gtrsim 1$. Therefore, in order to satisfy constraints on $\Omega_{\text{DM}}^{(0)}$ (as well as z_{eq}),

one must introduce a second DM component, which is non-interacting and dominates for most of the history.

Finally, we note that while Eq. (30) is an extra tuning on $V(\phi)$, normal quintessence also suffers from the same constraint. Indeed, “tracker” quintessence with $V(\phi) = M^4(M_{\text{Pl}}/\phi)^\alpha$ leads to a dark energy equation of state

$$w_\phi = -\frac{2}{\alpha + 2}. \quad (31)$$

Imposing the current observational constraint $w < -0.9$ results in a bound on α identical to Eq. (30).

B. CMB and SNIa observables

We now focus on cosmological distance tests, in particular the SNIa luminosity-distance relation and the angular-diameter distance to the last scattering surface as inferred from the position of CMB acoustic peaks. We wish to compare these observables for three different models, namely the interacting scalar field dark matter model with $\alpha = 0.2$ and $\beta = 1$, a Λ CDM model, and a phantom model with $w = -1.2$.

The position of Doppler peaks depends on the angular-diameter distance to the last scattering surface,

$$d_A(z_{\text{rec}}) = (1 + z_{\text{rec}})^{-1} \int_0^{z_{\text{rec}}} \frac{dz}{H(z)}, \quad (32)$$

where z_{rec} is the redshift at recombination. Observations of SNIa, on the other hand, probe the luminosity distance

$$d_L(z) = (1 + z) \int_0^z \frac{dz}{H(z)}. \quad (33)$$

Figure 2a shows the luminosity distance for all three models with $\Omega_{\text{DM}}^{(0)} = 0.3$, while Fig. 2b gives their percentage difference. The difference between our model and Λ CDM is $\lesssim 4\%$ for $z < 1.5$; similarly the difference with respect to the phantom model is within $\lesssim 2\%$. Thus all three models are degenerate within the uncertainties of present SNIa data which determine $d_L(z)$ to no better than $\sim 7\%$. Furthermore, this suggests that percent-level accuracy from future SNIa experiments such as the Supernova Acceleration Probe (SNAP) [29], combined with other cosmological probes, could distinguish between them.

Since $\Omega_{\text{DM}}^{(0)}$ is kept fixed in this case, the matter density in the interacting dark energy model differs in the past from that in the Λ CDM and phantom cases, as seen from Eq. (29). This results in a 10% difference in $d_A(z_{\text{rec}})$, which is again within current CMB uncertainties.

Suppose we instead keep $d_A(z_{\text{rec}})$ fixed, which essentially amounts to fixing the matter density at high redshift. With $\Omega_{\text{DM}}^{(0)} = 0.3$ for both the Λ CDM and phantom models, this is achieved by setting $\Omega_{\text{DM}}^{(0)} = 0.4$ for our model. These values are compatible with current limits, as mentioned earlier. The resulting luminosity distances

and percentage differences are plotted in Fig. 3. In this case we find that our model is more closely degenerate with Λ CDM than phantom.

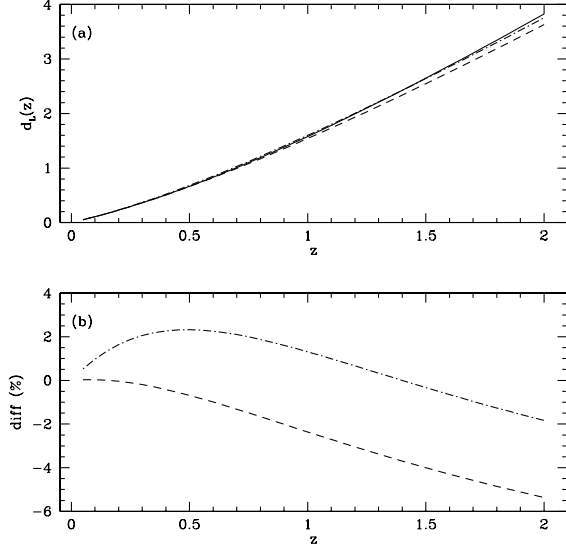


FIG. 2: Upper panel shows the luminosity distance (d_L) as function of redshift for our model (solid) a phantom model with $w = -1.2$ (dash-dot) and Λ CDM (dash). We have fixed $\Omega_{\text{DM}}^{(0)} = 0.3$. Lower panel shows the percentage difference between our model and phantom (dash-dot), and between our model and Λ CDM (dash), respectively.

C. Growth of density perturbations

In the slow-roll approximation the evolution equation for dark matter inhomogeneities, $\delta = \delta\rho_{\text{DM}}/\rho_{\text{DM}}$, is given in synchronous gauge by [16]

$$\delta'' + aH\delta' = \frac{3}{2}a^2H^2 \left[1 + \frac{2\beta^2}{1 + a^2V_{,\phi\phi}/k^2} \right] \delta, \quad (34)$$

where primes denote differentiation with respect to conformal time. This differs from the corresponding expression in CDM models only through the factor in square brackets, normally equal to unity. Since this term accounts for the self-attractive force on the perturbation, the extra contribution proportional to β^2 arises from the attractive fifth force mediated by the scalar field. This force has a finite range, which for an inverse power-law potential is

$$\lambda = V_{,\phi\phi}^{-1/2} = \sqrt{\frac{\phi^{\alpha+2}}{\alpha(\alpha+1)M^4M_{\text{Pl}}^\alpha}}. \quad (35)$$

Perturbations with physical wavelength much larger than λ , *i.e.* $a/k \gg \lambda$, evolve as normal CDM. On the other hand, perturbations with $a/k \ll \lambda$, evolve as if

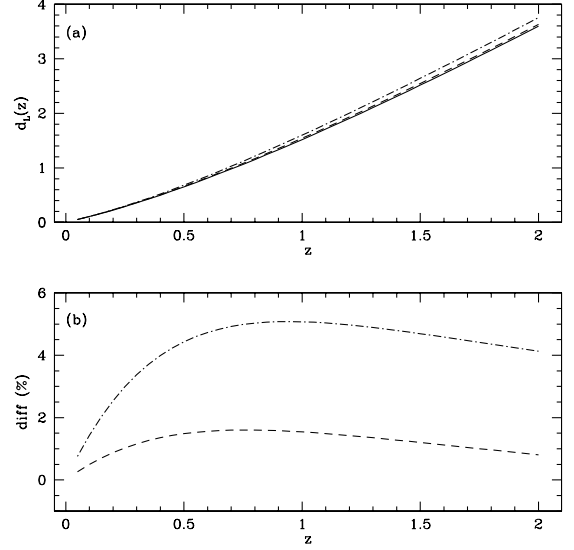


FIG. 3: Same as in Figure 2, except $\Omega_{\text{DM}}^{(0)} = 0.4$ for the interacting scalar field dark matter model in this case. This gives equal $d_A(z_{\text{rec}})$ for all three models.

Newton's constant were a factor of $1 + 2\beta^2$ larger. Thus the interaction with the quintessence field leads to an enhancement of power on small scales [30]. In particular, small-scale perturbations go non-linear at higher redshift than in Λ CDM, as shown recently in a closely related context of chameleon cosmology [31]. (Numerical simulations have also found that a similar attractive scalar interaction for dark matter particles, albeit with a much smaller range of 1 Mpc, results in emptier voids between concentrations of large galaxies [32].)

Quantitatively, from Eqs. (23) and (24) in the limit $\alpha \ll 1$, we obtain

$$V_{,\phi\phi} \approx H_0^2(1+z)^6 e^{2\beta(\phi-\phi_0)/M_{\text{Pl}}} \frac{3\beta^2}{\alpha} \frac{(\Omega_{\text{DM}}^{(0)})^2}{\Omega_{\text{DE}}^{(0)}}, \quad (36)$$

where H_0 is the present value of the Hubble parameter. This implies, for instance, that at the present epoch

$$\lambda^{(0)} = H_0^{-1} \sqrt{\frac{\alpha\Omega_{\text{DE}}^{(0)}}{3\beta^2(\Omega_{\text{DM}}^{(0)})^2}} \approx 0.7H_0^{-1}, \quad (37)$$

where in the last step we have taken $\alpha = 0.2$, $\beta = 1$ and $\Omega_{\text{DM}}^{(0)} = 0.3$. Hence the present range of this fifth force is comparable to the size of the observable universe. However, λ varies with redshift, and it is easily seen that $\lambda \ll H^{-1}$ in the past. In particular, we do not expect measurable effects in the CMB. This is in contrast with quintessence models [4], as well as the interacting dark matter/dark energy model of Amendola and collaborators [14], where $m \sim H$ along the attractor solution, leading to imprints in the CMB.

We solve numerically Eq. (34) and compute the linear matter power spectrum, $\Delta^2(k) \propto k^3 P(k)$, normalized to WMAP [26], where $P(k) = |\delta_k|^2$. In Fig. 4a we plot the resulting power spectrum for our model (solid line) and ΛCDM (dash line) with $\Omega_{\text{DM}}^{(0)} = 0.4$ and 0.3 respectively. The two curves are essentially indistinguishable by eye.

In Fig. 4b we plot the fractional difference between the two spectra. The discrepancy is $< 2\%$ on the scales probed by current large scale structure surveys and consistent with the experimental accuracy of 2dF Galaxy Redshift Survey [27] and Sloan Digital Sky Survey (SDSS) [33]. On large scales the perturbations in the two models evolve in a similar way ($k < 0.01 \text{ hMpc}^{-1}$), while on intermediate scales ($0.01 < k < 0.4 \text{ hMpc}^{-1}$) the ΛCDM shows a few percent excess of power which is mostly due to small difference in the expansion rate of the two models after decoupling. Most importantly, on smaller scales ($k > 0.4 \text{ hMpc}^{-1}$) the power spectrum of ΛCDM is suppressed compared to our model. This is due to the fifth force which enhances the clustering of dark matter perturbations compared to the uncoupled case. However, in this range perturbations become non-linear; hence a rigorous study of how this fifth force affects structure formation requires N-body simulations.

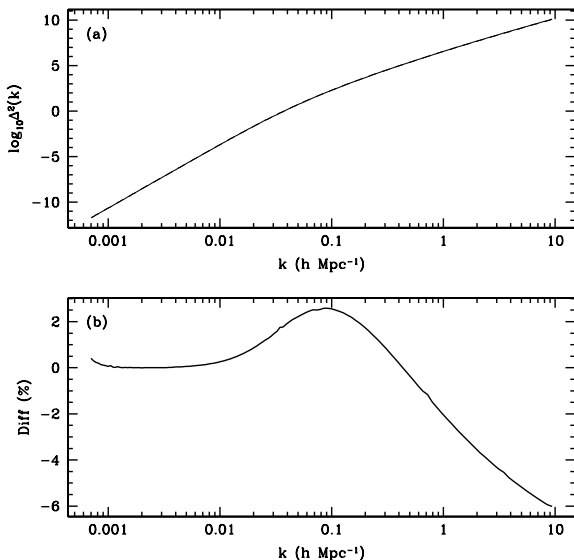


FIG. 4: Upper panel shows the matter power spectrum ($\Delta^2(k)$) over the relevant range of scales for our model (solid) and ΛCDM (dash) with $\Omega_{\text{DM}}^{(0)} = 0.4$ and 0.3 , respectively. Lower panel shows the percentage difference between the two curves, which is well within current experimental accuracy.

D. Galaxy and cluster dynamics

Since the ϕ -mediated force is long-range today (see Eq. (37)), our model is subject to constraints from galaxy

and cluster dynamics [30]. For instance, a fifth force in the dark sector leads to a discrepancy in mass estimates of a cluster acting as a strong lens for a high-redshift galaxy. Lensing measurements probe the actual mass since photons are oblivious to the fifth force, while dynamical observations are affected and would overestimate the mass of the cluster.

Other effects studied in [30] include mass-to-light ratios in the Local Group, rotation curves of galaxies in clusters, and dynamics of rich clusters. These combine to yield a constraint of $\beta \lesssim 0.8$, consistent with our assumption of $\beta \sim \mathcal{O}(1)$. This is consistent with generic string compactifications; if for instance ϕ is the radion field measuring the distance between two end-of-the-world branes, $\beta = 1/\sqrt{6}$ [16].

VI. DISCUSSION

In this paper we have shown that an interaction between dark matter and dark energy generically mimics $w < -1$ cosmology, provided that the observer treats the dark matter as non-interacting. Unlike phantom models, the theory is well-defined and free of ghosts.

Our model is consistent with current observations provided the scalar potential is sufficiently flat. For our fiducial $V(\phi) = M^4/\phi^\alpha$, this translates into $\alpha \lesssim 0.2$. This is no worse than normal quintessence with tracker potential, where a nearly identical bound follows from observational constraints on w_ϕ .

In fact our scenario is less constrained than other interacting dark energy/dark matter models studied in the literature. There is no need to introduce a non-interacting DM component, as in [19]; nor does the coupling strength need be much weaker than gravity, $\beta \lesssim 0.1$, as in [14]. Instead, our model allows for a single interacting DM species with gravitational strength coupling to dark energy — $\beta \sim \mathcal{O}(1)$. In both cases this traces back to a difference in attractor solutions.

At the level of current uncertainties, the model is degenerate with both ΛCDM and phantom models. However, our calculations of luminosity and angular-diameter distances indicate that these models could be distinguished by the next generation of cosmological experiments devoted to the study of dark energy, such as SNAP, the Large Synoptic Survey Telescope (LSST) [34], the Joint Efficient Dark-energy Investigation (JEDI) [35], the Advanced Liquid-mirror Probe for Astrophysics, Cosmology and Asteroids (ALPACA) [36], and others.

A dark sector interaction may reveal itself in various ways in the data. A strong hint would be a preference for $w < -1$ when fitting cosmological distance measurements assuming CDM. Another indication is a discrepancy between the clustering matter density at various redshifts and the expected $(1+z)^3$ dependence in normal CDM models, which could appear as a discrepancy in the inferred value of $\Omega_M^{(0)}$.

We also uncovered modifications in the linear matter

power spectrum and large-scale structure. These are primarily due to the attractive scalar-mediated force which enhances the growth of DM perturbations on small scales. Note that the opposite behavior obtains for a phantom scalar coupled to dark matter, resulting in a repulsive scalar force which damps perturbations [37]. As mentioned earlier, non-linear effects are important for the relevant range of scales and would require N-body simulations.

Other observational effects that could distinguish our model from Λ CDM and phantom include the bias parameter. Since baryons are unaffected by the fifth force, baryon fluctuations develop a constant large-scale bias [38] which could be observable. Similarly, comparison of the redshift dependence of the matter power spectrum, $P(k, z)$, may be useful to constrain the scale λ , which varies with z . The integrated Sachs-Wolfe effect is another mechanism worth studying. Since the present

range of our scalar force is comparable to the size of the observable universe, it might account for the observed lack of power on large scales in the CMB.

Acknowledgments

We are grateful to L. Amendola, R. Caldwell, E. Copeland, G. Huey, M. Trodden, B. Wandelt and N. Weiner for insightful comments. S.D. is thankful to L. Hui for support under DOE grant number DE-FG02-92-ER40699 and B. Greene for the opportunity to work at ISCAP. This work is supported in part by the Columbia Academic Quality Funds (P.S.C.) and the U.S. Department of Energy under cooperative research agreement DE-FC02-94ER40818 (J.K.).

[1] U. Seljak *et al.*, Phys. Rev. D **71**, 103515 (2005).
[2] S. Weinberg, Phys. Rev. Lett. **59**, 2607 (1987).
[3] C. Wetterich, Nucl. Phys. **B302**, 668 (1988); P.J.E. Peebles and B. Ratra, ApJ **325**, L17 (1988).
[4] R.R. Caldwell, R. Dave and P.J. Steinhardt, Phys. Rev. Lett. **80**, 1582 (1998).
[5] U. Alam, V. Sahni, T.D. Saini and A.A. Starobinsky, Mon. Not. Roy. Astron. Soc. **354**, 275 (2004); D. Huterer and A. Cooray, Phys. Rev. D **71**, 023506 (2005); B.A. Bassett, P.S. Corasaniti and M. Kunz, Astrophys. J. **617**, L1 (2004); E. Majerotto, D. Sapone and L. Amendola, astro-ph/0410543.
[6] P.S. Corasaniti, M. Kunz, D. Parkinson, E.J. Copeland and B.A. Bassett, Phys. Rev. D **70**, 083006 (2004).
[7] A.G. Riess *et al.*, Astrophys. J. **607**, 665 (2004).
[8] I. Maor, R. Brustein, J. McMahon and P.J. Steinhardt, Phys. Rev. D **65**, 123003 (2002).
[9] R.R. Caldwell, M. Kamionkowski and N.N. Weinberg, Phys. Rev. Lett. **91**, 071301 (2003).
[10] S.M. Carroll, M. Hoffman and M. Trodden, Phys. Rev. D **68**, 023509 (2003); J.M. Cline, S.Y. Jeon and G.D. Moore, Phys. Rev. D **70**, 043543 (2004); S.D.H. Hsu, A. Jenkins and M.B. Wise, Phys. Lett. B **597**, 270 (2004).
[11] D.F. Torres, Phys. Rev. D **66**, 043522 (2002); S. Capozziello, Int. Journ. Mod. Phys. **11**, 483 (2002); S. M. Carroll, A. De Felice and M. Trodden, Phys. Rev. D **71**, 023525 (2005); V. Faraoni, Phys. Rev. D **68**, 063508 (2003); G. Allemandi, A. Borowiec and M. Francaviglia, Phys. Rev. D **70**, 103503 (2004).
[12] C. Csaki, N. Kaloper and J. Terning, Annals Phys. **317**, 410 (2005), astro-ph/0409596.
[13] T. Damour, G.W. Gibbons and C. Gundlach, Phys. Rev. Lett. **64**, 123 (1990); J.A. Casas, J. Garcia-Bellido and M. Quiros, Clas. Quant. Grav. **9**, 1371 (1992); R. Bean, Phys. Rev. D **64**, 123516 (2001); D. Comelli, M. Pietroni and A. Riotto, Phys. Lett. B **571**, 115 (2003);
[14] L. Amendola, Phys. Rev. D **62**, 043511 (2000); L. Amendola and D. Tocchini-Valentini, Phys. Rev. D **64**, 043509 (2001); L. Amendola, C. Quercellini, D. Tocchini-Valentini and A. Pasqui, Astrophys. J. **583**, L53 (2003); L. Amendola and C. Quercellini, Phys. Rev. D **68**, 023514 (2003).
[15] J. Khoury and A. Weltman, Phys. Rev. Lett. **93**, 172204 (2004); Phys. Rev. D **69**, 044026 (2004); S.S. Gubser and J. Khoury, Phys. Rev. D **70**, 104001 (2004).
[16] P. Brax, C. van de Bruck, A.C. Davis, J. Khoury and A. Weltman, Phys. Rev. D **70**, 123518 (2004); astro-ph/0410103.
[17] G.R. Farrar and P.J.E. Peebles, Astrophys. J. **604**, 1 (2004); S.S. Gubser and P.J.E. Peebles, Phys. Rev. D **70**, 123510 (2004).
[18] D.B. Kaplan, A.E. Nelson and N. Weiner, Phys. Rev. Lett. **93**, 091801 (2004); R. D. Peccei, Phys. Rev. D **71**, 023527 (2005).
[19] G. Huey and B.D. Wandelt, astro-ph/0407196.
[20] P.J. Steinhardt, L. Wang and I. Zlatev, Phys. Rev. D **59**, 123504 (1999).
[21] G.W. Anderson and S.M. Carroll, astro-ph/9711288.
[22] T. Damour and A.M. Polyakov, Nucl. Phys. **B423**, 532 (1994); T. Damour and A.M. Polyakov, Gen. Rel. Grav. **26**, 1171 (1994).
[23] G. Huey, P.J. Steinhardt, B.A. Ovrut and D. Waldram, Phys. Lett. B **476**, 379 (2000); C.T. Hill and G.C. Ross, Nucl. Phys. **B311**, 253 (1988); J. Ellis, S. Kalaru, K.A. Olive and C. Wetterich, Phys. Lett. B **228**, 264 (1989).
[24] T. Biswas and A. Mazumdar, hep-th/0408026.
[25] M. Kunz, P.S. Corasaniti, D. Parkinson and E.J. Copeland, Phys. Rev. D **70**, 041301 (2004).
[26] H. V. Peiris *et al.*, Astrophys. J. Suppl. **148**, 213 (2003).
[27] W. J. Percival *et al.* [The 2dFGRS Collaboration], Mon. Not. Roy. Astron. Soc. **327**, 1297 (2001); S. Cole *et al.* [The 2dFGRS Collaboration], Mon. Not. Roy. Astron. Soc. **362** (2005) 505.
[28] S. Hannestad and E. Mortsell, JCAP **09**, 001 (2004); D. Rapetti, S.W. Allen and J. Weller, Mon. Not. Roy. Astron. Soc. **360**, 555 (2005).
[29] G. Aldering [SNAP Collaboration], astro-ph/0209550.
[30] B. A. Gradwohl and J. A. Frieman, Astrophys. J. **398**, 407 (1992).

- [31] P. Brax, C. van de Bruck, A.C. Davis and A.M. Green, [astro-ph/0509878](http://arxiv.org/abs/astro-ph/0509878).
- [32] A. Nusser, S. S. Gubser and P. J. E. Peebles, Phys. Rev. D **71**, 083505 (2005).
- [33] M. Tegmark *et al.* [SDSS Collaboration], Astrophys. J. **606**, 702 (2004).
- [34] See <http://www.lsst.org>.
- [35] A. Croots *et al.*, [astro-ph/0507043](http://arxiv.org/abs/astro-ph/0507043).
- [36] See <http://www.astro.ubc.ca/LMT/almaca/>.
- [37] L. Amendola, Phys. Rev. Lett. **93**, 181102 (2004); L. Amendola, S. Tsujikawa and M. Sami, [astro-ph/0506222](http://arxiv.org/abs/astro-ph/0506222).
- [38] L. Amendola and D. Tocchini-Valentini, Phys. Rev. D **66**, 043528 (2002).